JOURNAL OF PETROLOGY | VOLUME 41 | NUMBER 7 | PAGES 933–950 | 2000

On and Off the North China Craton: Where is the Archaean Keel?

W. M. FAN[1,2], H. F. ZHANG[1,3], J. BAKER[1,4], K. E. JARVIS[5], P. R. D. MASON[6] AND M. A. MENZIES[1]*

[1]DEPARTMENT OF GEOLOGY, ROYAL HOLLOWAY UNIVERSITY OF LONDON, EGHAM TW20 OEX, UK

[2]CHANGSHA INSTITUTE OF GEOTECTONICS, ACADEMIA SINICA, CHANGSHA, HUNAN 410013, P.R. CHINA

[3]INSTITUTE OF GEOLOGY AND GEOPHYSICS, CHINESE ACADEMY OF SCIENCES, BEIJING 100029, P.R. CHINA

[4]DANISH LITHOSPHERE CENTRE, 10 ØSTER VOLDGADE, 1350 KØBENHAVN, DENMARK

[5]KINGSTON UNIVERSITY, PENRHYN ROAD, KINGSTON UPON THAMES KT1 2EE, UK

[6]VENING MEINESZ SCHOOL OF GEODYNAMICS, UTRECHT UNIVERSITY, 3508 TA UTRECHT, NETHERLANDS

RECEIVED JUNE 11, 1999; REVISED TYPESCRIPT ACCEPTED FEBRUARY 18, 2000

Geophysical data indicate that the lithosphere beneath the North China Craton (NCC) is ~80 km thick with high heat flow within the craton. This is somewhat in disagreement with the presence of Archaean crustal rocks and kimberlite-hosted xenoliths that point to the existence of garnet–diamond-facies mantle beneath the craton, as recently as the Ordovician. Basalt-hosted mantle xenoliths entrained during the Cenozoic may provide a clue to Phanerozoic changes. Of particular note is the predominance of spinel-facies peridotites (75–80 km) and the paucity of garnet-facies peridotites. The modal mineralogy of the spinel peridotites is similar to that observed in peridotite xenoliths from the lower oceanic lithosphere but distinct from that of abyssal peridotites. The orthopyroxene/olivine ratio is like that of peridotites from ocean basins and tectonically active continents, and the peridotites have 'depleted' Sr and Nd isotopic ratios similar to those of oceanic basalts. The basalt-hosted xenolith data from eastern China support geophysical data in revealing the presence of thin, hot lithosphere with a similarity, over distances of several thousand kilometres, to that found beneath tectonically active continents or ocean basins. These data do not, however, allow us to constrain which of the thermotectonic processes (i.e. plume, extension, delamination) was responsible for the loss of the cold, thick Archaean lithospheric root (~200 km) in the last 400 my. What is clear is that the preexistent, presumably heterogeneous, Archaean lithosphere has been very effectively replaced by 'oceanic'-like mantle. The extent to which it was totally replaced is open to debate.

KEY WORDS: *North China Craton; mantle xenoliths; oceanic affinity*

INTRODUCTION

Traditionally cratons are thought of as parts of the continental lithosphere in which Archaean crustal rocks are exposed at the Earth's surface and where thermal and tectonic events occurred >2500 my ago. One of the best studied examples is the Kaapvaal craton, South Africa. Aspects of the petrology and geochemistry of kimberlite-hosted mantle xenoliths indicate that areas of Archaean crust are underlain by refractory peridotites (e.g. Cox *et al.*, 1973; Boyd & Nixon, 1978; Erlank *et al.*, 1987). Geochronology and geochemistry have demonstrated the presence of ancient enriched mantle, coupled crust–mantle evolution, and tectonic and thermal stability for 3–4 by (Menzies & Murthy 1980; Walker *et al.*, 1989; Hawkesworth *et al.*, 1990; Carlson & Irving, 1994; Pearson *et al.*, 1995*a*, 1995*b*). Silicate inclusions in megacrystic diamonds found in kimberlites reveal that a considerable thickness of lithosphere (~200 km) formed in the first billion years of Earth's history perhaps as a result of high thermal gradients and greater melt production (e.g. Richardson *et al.*, 1984, 1993; Boyd *et al.*, 1985). Seismic data indicate a high-velocity seismic lid imaged to depths of several hundred kilometres (i.e. 150–250 km) verifying the long-term stability and relative inertness of cratons (e.g. Jordan, 1988; Polet & Anderson, 1995; Van Der Lee & Nolet, 1997).

*Corresponding author. e-mail: menzies@gl.rhbnc.ac.uk

Until recently, petrological and chemical studies of on-craton peridotites revealed that cratonic mantle was chemically distinctive compared with peridotites from other tectonic settings such as the ocean basins and tectonically active continents (e.g. Boyd, 1989). For example, the petrology and geochemistry of xenoliths from the Siberian craton is similar to that of xenoliths from the Kaapvaal craton (Griffin *et al.*, 1996; Boyd *et al.*, 1997). However, craton–shield areas within Canada and Tanzania (Rudnick *et al.*, 1994; Kelemen *et al.*, 1998; Griffin *et al.*, 1999*a*, 1999*b*; Lee & Rudnick, 2000) do not have the restricted range in olivine composition and the orthopyroxene/olivine ratio reported from the Kaapvaal craton (Boyd, 1989). Although Griffin *et al.* (1999*a*) cautioned against over-interpretation on the basis of limited samples, the most recent database for cratons such as Tanzania (e.g. Rudnick *et al.*, 1994; Lee & Rudnick, 2000) indicates that the evolutionary history of some of the world's cratons is different from that of Kaapvaal (Boyd, 1989). Griffin *et al.* (1999*a*, 1999*b*) proposed that the shallow sub-cratonic mantle beneath Canada was accreted above ancient subduction zones, hence the similarity with modern (<200 Ma) arc peridotites (Kelemen *et al.*, 1998). Petrogenetic models founded on the belief that higher thermal gradients in the Archaean produced highly refractory residues (e.g. Hanson & Langmuir, 1978; Boyd, 1989; Walker *et al.*, 1989) are now balanced by models invoking fluid processes as the mechanism for producing highly refractory residues (e.g. supra-subduction zone). Rudnick *et al.* (1994) and Kelemen *et al.* (1998) attributed the magnesian nature of cratonic peridotites to the interaction of silica-rich liquids with low orthopyroxene magnesian peridotites producing orthopyroxene-rich peridotites.

Several Archaean areas are not underlain by a clearly defined seismic lid reaching several hundred kilometres into the upper mantle (Anderson *et al.*, 1992; Grand, 1994). For example, the Hebridean craton of NW Scotland (Menzies & Halliday, 1988) has a thickness of ~80 km because it is part of the rifted volcanic margin of the North Atlantic Ocean and may have been thermally thinned by the Iceland plume. Similarly, the Arabian craton has exposures of Archaean crustal rocks (Whitehouse *et al.*, 1994) with a lithosphere thickness of <100 km, perhaps because this is part of the rifted margin of the Red Sea–Gulf of Aden influenced by the Afar plume. Also, the seismic character of the mantle beneath the Slave Province, Canada, is different from that of the Kaapvaal and Siberian cratons, and there is some debate as to whether or not a high- or low-velocity structure exists beneath the craton (Hoffman, 1990).

In this paper we investigate the North China Craton and off-craton mobile belts of eastern China. The North China Craton (NCC) is characterized by late Archaean crustal rocks and has been intruded by Ordovician diamondiferous kimberlites and Cenozoic alkali basalts (Chi *et al.*, 1992) both containing mantle xenoliths. Basalt-hosted spinel-facies mantle rocks are used to investigate the nature of the shallow mantle and these data are compared with data from other tectonic settings. This includes (1) Archaean cratons [e.g. Africa (Kaapvaal and Tanzania), North America, Greenland], (2) tectonically active continents (e.g. Basin and Range, North America), and (3) modern ocean basins (e.g. Atlantic Ocean). This study addresses the following questions. What is the nature of the uppermost mantle beneath eastern China? Does on- and off-craton provinciality exist as it does in other parts of the world? Which processes best account for the formation of the lithospheric mantle beneath eastern China? How does present-day lithosphere compare with the Archaean lithosphere known to have survived until the Ordovician?

GEOLOGICAL BACKGROUND

The North China Craton (NCC) is composed of Archaean and Proterozoic metamorphic rocks with the oldest recorded crustal ages being ~3·8 Ga (Liu *et al.*, 1992). The cratonic nucleus is surrounded by three tectonically different regions from north to south, the NE China fold belts (Variscan), the Yangtze craton (Proterozoic) and the SE China fold system (Caledonian). The cratonic nucleus and the surrounding terranes have been intruded by kimberlites and basalts that have entrained fragments of the sub-crustal mantle at discrete periods during the Phanerozoic (Griffin *et al.*, 1998; X. Xu *et al.*, 1998). Several kimberlites (Chi *et al.*, 1992) are reported from within the Archaean crust at Mengyin, Shandong province, and at Fuxian, Liaoning province (Fig. 1). The diamondiferous character of some of the kimberlite pipes and the predominance of P-type inclusions (i.e. peridotite) in diamonds (e.g. Chi *et al.*, 1992) suggests that the early Phanerozoic lithosphere was thick and stable to depths within the diamond stability field (i.e. 180–200 km). Later eruption of post-Cretaceous rift-related basalts entrained shallow mantle rocks (e.g. Song & Frey, 1989; Tatsumoto *et al.*, 1992) and thus provided two time windows on the nature of the mantle beneath the NCC (Menzies *et al.*, 1993; Griffin *et al.*, 1998). On- and off-craton lithosphere provinciality can best be investigated using Cenozoic xenolith-bearing basalts erupted along major lithospheric fault systems, through lithosphere of variable age, thickness and heat flow (e.g. Zhou & Armstrong, 1982; Peng *et al.*, 1986; Zhi *et al.*, 1990; Fan & Hooper, 1991; Zhang *et al.*, 1991; Deng & Macdougall, 1992; Tatsumoto *et al.*, 1992; Zhou & Zhu, 1992; Qi *et al.*, 1995; Y. Xu *et al.*, 1996, 1998; X. Xu *et al.*, 1998).

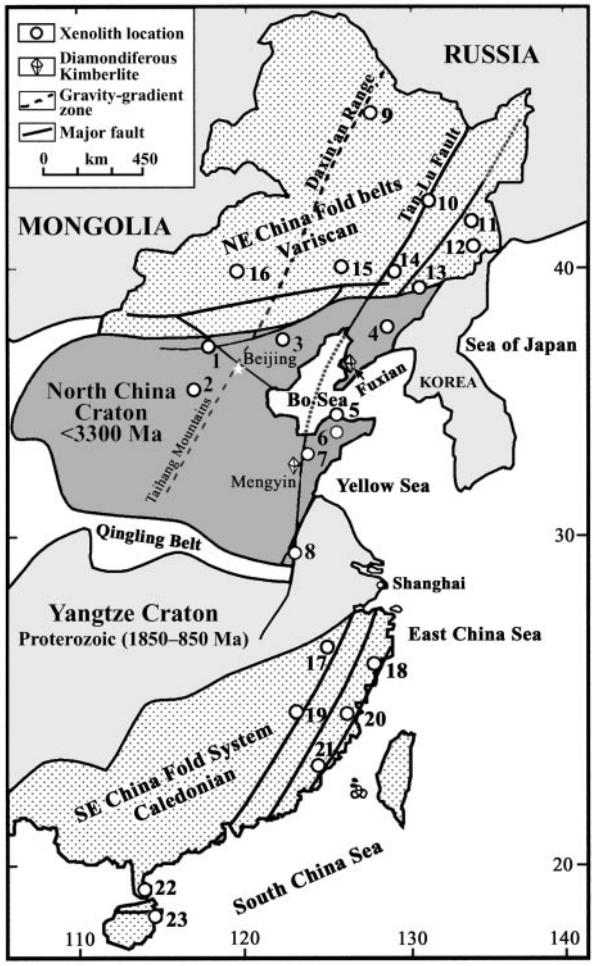

Fig. 1. Simplified tectonic map of eastern China [after Ma & Wu (1981)] with basalt-hosted xenolith localities shown as numbers and kimberlite-hosted xenolith localities as diamonds. Basalt-hosted peridotite xenoliths were collected from on- and off-craton localities where basalts had entrained xenoliths erupted through Archaean (i.e. North China Craton) and post-Archaean crust (i.e. NE China fold belts; Yangtze craton and SE China fold system). On-craton localities: 1, Hannuoba; 2, Fansi; 3, Pingquan; 4, Kuandian; 5, Penglai; 6, Qixia; 7, Linqu; 8, Jiashan. Off-craton localities: 9, Wudalianchi; 10, Shangzhi; 11, Jingbohu; 12, Wangqing; 13, Huinan; 14, Yitong; 15, Abaga; 16, Shuangliao; 17, Xilong; 18, Ninghai; 19, Mingxi; 20, Minqing; 21, Longhai; 22, Xuwen; 23, Wenchang.

ANALYTICAL TECHNIQUES

Representative spinel-facies peridotites were selected from several 'on-craton' (i.e. Hannuoba, Fansi, Linqu, Qixia, Penglai) and 'off-craton' (i.e. Yitong, Shangzhi, Shuangliao, Huinan, Ninghai, Xilong, Xuwen, Wenchang) (Fig. 1) localities. The modal mineralogy of the peridotites is based on spot counting of >1000 grains (Table 1; Fig. 2). Xenoliths were crushed to <30 mesh and clear olivines were carefully hand-picked under a binocular microscope. Clean olivines were mounted onto a glass holder and then surface-polished. Olivine major element compositions were determined at the Department of Geology, Birkbeck College, University of London, using a JEOL Superprobe equipped with an automated (AN 10000/55S with 2500 CPS) energy-dispersive system (EDS). Analyses were performed with a beam of 15 keV and 15 nA focused to a spot of ~1 μm diameter. ZAF4 and a cobalt standard were used for the on-line correction and the spectrum calibration. Analytical uncertainties for major elements were estimated at the level of <1% with the majority between 0·2 and 0·5% (Table 2).

Hand-picked clinopyroxene separates (~200 mg), without visible inclusions, were leached with hot 6 M sub-boiled HCl for 30 min and dissolved in distilled $HF–HNO_3$ and 6 M HCl in Savillex screwtop capsules at 150°C for 4–6 days. Each dissolved sample was split into two aliquots; one was used for trace element determination diluted to ~5000 times before analysis and the other was used for the determination of Sr and Nd isotope composition. Trace elements in clinopyroxenes were measured at CARE Imperial College (Silwood Park, Ascot) by inductively coupled plasma-mass spectrometry (ICP-MS) (Table 3). A blank was processed with each set of 11 samples and blanks for most of the elements were <0·05 ppm. To monitor precision, three duplicates and three standards (i.e. BEN, NIMN, BHVO-1) were prepared using the same procedures. This standard and blank data are given in Table 4. The discrepancy between duplicates was <10% for the majority of elements and analyses of standards are very close to the recommended values with most elements <5% (Table 3).

RESULTS

Clinopyroxene:orthopyroxene:olivine modes

The majority of the basalt-hosted xenoliths from eastern China are spinel-facies peridotites. On the basis of available samples both on-craton and off-craton localities (Fig. 2) are predominantly spinel lherzolites with essentially the same mineralogy and only slight variations in their clinopyroxene/orthopyroxene ratio. For the xenoliths from eastern China the modal compositions converge on an average composition of 64% olivine, 20% orthopyroxene, 14% clinopyroxene and 2% spinel. The modal mineralogy of the peridotites illustrates no real difference between on- and off-craton occurrences (Fig. 2).

Comparison of the mineral modes of the Chinese mantle rocks with a selection of on-craton data from elsewhere indicates some marked differences. On-craton (>2500 Ma), low-temperature peridotites from South Africa (Kaapvaal) tend to have a greater range in olivine/orthopyroxene ratio and to be clinopyroxene

Table 1: Estimated mineral abundances of eastern China spinel-facies mantle xenoliths (normalized to 100%)

Locality	Sample	Lithos	OL	OPX	CPX	SP
On North China Craton						
Hannuoba	92HD-01	SP lherzolite	76	14	8	2
Hannuoba	92HD-02	OL websterite	18	70	10	2
Fansi	SF-20	SP lherzolite	57	13	28	2
Fansi	SF-21	Pyroxenite	60	26	13	1
Linqu	92LQ-01	SP lherzolite	70	10	14	6
Linqu	92LQ-02	SP lherzolite	67	8	22	3
Linqu	92LQ-04	SP lherzolite	63	22	13	2
Linqu	92LQ-09	SP lherzolite	62	10	26	2
Penglai	92PL-01	SP lherzolite	55	12	31	2
Penglai	92PL-07	SP lherzolite	60	8	29	3
Penglai	92PL-36	SP lherzolite	63	8	28	1
Qixia	92QX-02	OL websterite	20	68	10	2
Qixia	92QX-03	OL websterite	21	70	8	1
Qixia	92QX-04	SP lherzolite	71	19	7	3
Qixia	92QX-05	SP lherzolite	71	20	8	1
Qixia	92QX-06	SP lherzolite	72	20	8	0
Off-craton NE and SE China fold belts						
Shangliao	92SL-01	SP lherzolite	58	30	10	2
Shangliao	92SL-02	SP lherzolite	63	29	6	2
Shangliao	92SL-04	SP lherzolite	60	14	25	1
Shangliao	92SL-13	SP lherzolite	61	24	13	2
Shangliao	92SL-14	SP lherzolite	62	30	6	2
Huinan	92HN-07	SP lherzolite	60	28	10	2
Huinan	92HN-09	SP lherzolite	61	23	14	2
Huinan	92HN-11	SP lherzolite	53	28	15	4
Huinan	92HN-16	SP lherzolite	54	30	14	2
Huinan	92HN-21	OL websterite	22	15	60	3
Yitong	92YT-01	SP lherzolite	71	18	10	1
Yitong	92YT-03	SP lherzolite	63	25	11	1
Yitong	92YT-04	OL websterite	24	12	63	1
Yitong	92YT-07	SP lherzolite	66	25	8	1
Yitong	92YT-10	OL websterite	20	10	70	0
Shangzhi	92SZ-01	SP lherzolite	64	23	12	1
Shangzhi	92SZ-02	SP lherzolite	69	21	8	2
Shangzhi	92SZ-03	SP lherzolite	68	20	9	3
Shangzhi	92SZ-04	SP lherzolite	64	15	19	2
Xilong	92XL-01	SP lherzolite	62	27	10	1
Xilong	92XL-02	SP lherzolite	68	19	11	2
Xilong	92XL-04	SP lherzolite	61	23	14	2
Ninghai	1204-1-1	SP lherzolite	75	8	15	2
Xuwen	LTX-06	SP lherzolite	56	31	10	3
Wenchang	HPX-02	SP lherzolite	65	19	12	4
Wenchang	HPX-06	SP lherzolite	68	10	19	3
Wenchang	HPX-08	SP lherzolite	66	18	13	3

OL, olivine; OPX, orthopyroxene; CPX, clinopyroxene; SP, spinel.

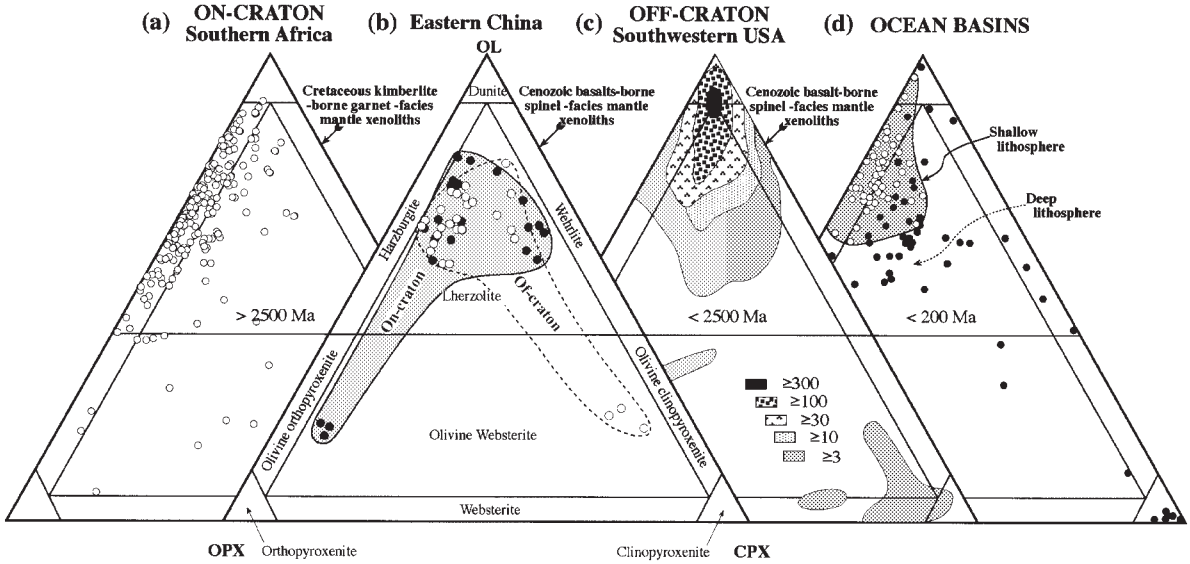

Fig. 2. Petrological classification of peridotites. On-craton: spinel- and garnet-facies peridotites from the Kaapvaal craton, South Africa. (Note that the majority of the rocks from the Kaapvaal craton are harzburgites.) Data are compiled from Carswell & Dawson (1970), Mathias *et al.* (1970), Chen (1971), Cox *et al.* (1973), Maaloe & Aoki (1977), Boyd & Nixon (1978), Dawson (1980) and Walker *et al.* (1989). Eastern China: spinel-facies mantle xenoliths entrained in Cenozoic basalts from on-craton and off-craton localities. Spinel lherzolite and olivine websterite xenoliths are found at on- and off-craton localities, indicating no marked provinciality in modal mineralogy. Unless otherwise stated these symbols are used in the same way in all the following figures. Off-craton: basalt-borne spinel-facies mantle xenoliths in Cenozoic basalts from a tectonically active continental margin—Basin and Range, SW USA [Menzies *et al.* (1987) and references therein]. These xenoliths are dominated by lherzolite and dunite, and so they are significantly different from the Kaapvaal craton, which is dominated by harzburgites. Ocean basins: oceanic peridotites are divided into shallow lithosphere (i.e. abyssal, ophiolitic) and deep lithosphere (i.e. basalt-borne xenoliths, Hawaii and Tahiti). These data point to the possible existence of 'layered oceanic lithosphere' with a shallow depleted layer (harzburgite–dunite) and a deeper less depleted layer (lherzolite) [Green *et al.* (1979) and references therein; Dick & Fisher (1984); Menzies (1991)]. It should be noted that the 'deep' basalt-borne xenoliths from ocean basins (i.e. deep lithosphere) are similar to those from eastern China.

poor (Fig. 2a) relative to the Chinese sub-Moho peridotites. It should be noted that the range in modal mineralogy for the Matsoku 'common' peridotites defined by Cox *et al.* (1973) (i.e. ol:opx:cpx:gt = 45–75%:20–50%:0–5%:0–11%) lies within the on-craton range (Fig. 2a). Comparison of off-craton (<2500 Ma) data with the Chinese mantle rocks indicates some marked similarities. Off-craton, high-temperature peridotites from the western USA (e.g. Basin and Range) tend to be more olivine rich with a greater propensity toward dunite–harzburgite modes (Fig. 2c). Lherzolites from eastern China tend to be similar in their mode to lherzolites from the Basin and Range, western USA. Oceanic peridotites (<200 Ma) from abyssal and basalt-hosted peridotites display a considerable range in modal mineralogy (Fig. 2d) with differences between shallow and deep lithospheric mantle that may point to it being 'stratified'. The shallow oceanic lithosphere, represented by abyssal, dredged and ophiolitic peridotites, tends to be clinopyroxene poor and dominated by harzburgites. In contrast, the deep oceanic lithosphere, represented by basalt-hosted xenoliths, tends to be more clinopyroxene rich and dominated by lherzolite. To complicate matters, the mode for shallow oceanic sub-Moho lithosphere overlaps with that for on-craton peridotites (see Kelemen *et al.*, 1998). The mode for deep lithospheric 'oceanic' mantle has some of the variation observed in both the eastern China mantle rocks and those from the Basin and Range. Basalt-hosted spinel-facies mantle xenoliths from Hawaii and Tahiti are similar, in their modal abundance, to the lower lithosphere beneath eastern China. In other words, it appears that mantle processes that produced the deep oceanic lithosphere beneath Hawaii and Tahiti (~100–150-my-old lithosphere) and tectonically active continental regions such as the Basin and Range may be similar to those processes responsible for the formation of part of the lithosphere beneath eastern China. In summary, the modal mineralogy of the Chinese xenoliths is very different from that of other Archaean cratons where garnet-facies harzburgites predominate. However, the Chinese xenoliths compare favourably with spinel-facies mantle xenoliths from

Table 2: Olivine major element compositions (wt %) in eastern China spinel-facies mantle xenoliths

Sample	SiO_2	Cr_2O_3	FeO	MnO	MgO	Total	Fo %
On North China Craton							
92HD-01	41·47	0·00	8·88	0·17	48·80	99·3	90·7
92HD-02	41·66	0·04	7·71	0·08	49·77	99·3	92·0
SF-20	41·22	0·07	10·16	0·10	48·07	99·6	89·4
SF-21	41·30	0·04	9·84	0·12	48·30	99·6	89·7
92LQ-02	41·69	0·05	8·90	0·14	48·97	99·8	90·7
92LQ-04	41·55	0·04	9·41	0·07	48·43	99·5	90·2
92PL-01	41·41	0·04	10·04	0·07	48·12	99·7	89·5
92PL-07	41·30	0·03	9·71	0·12	48·24	99·4	89·8
92PL-36	41·59	0·02	8·88	0·13	49·06	99·7	90·8
92QX-02	41·43	0·03	9·16	0·19	48·75	99·6	90·5
92QX-03	40·19	0·02	16·05	0·16	43·30	99·7	82·8
92QX-04	41·45	0·01	9·03	0·11	49·05	99·7	90·6
92QX-05	41·59	0·04	8·89	0·11	48·98	99·6	90·8
92QX-06	41·43	0·02	8·63	0·10	48·92	99·1	91·0
Off-craton NE and SE China fold belts							
92SL-01	41·50	0·05	9·84	0·12	48·09	99·6	89·7
92SL-02	41·78	0·01	8·54	0·09	49·18	99·6	91·1
92SL-04	41·64	0·01	9·50	0·12	48·45	99·7	90·1
92SL-13	41·53	0·01	9·25	0·07	48·56	99·4	90·3
92SL-14	41·70	0·01	8·69	0·07	49·22	99·7	91·0
92HN-07	41·37	0·02	9·70	0·16	48·53	99·8	89·9
92HN-09	41·37	0·01	9·57	0·12	48·55	99·6	90·0
92HN-11	41·13	0·04	10·70	0·11	47·49	99·5	88·8
92HN-16	41·37	0·04	9·97	0·14	48·08	99·6	89·6
92HN-21	41·05	0·03	11·96	0·16	46·52	99·7	87·4
92YT-01	41·46	0·02	9·21	0·08	48·60	99·4	90·4
92YT-03	41·26	0·05	11·02	0·08	47·21	99·6	88·4
92YT-04	41·62	0·01	9·47	0·17	48·54	99·8	90·1
92YT-07	41·40	0·03	9·88	0·14	48·36	99·8	89·7
92YT-10	41·05	0·03	11·40	0·18	47·04	99·7	88·0
92SZ-01	41·68	0·04	8·96	0·12	48·95	99·8	90·7
92SZ-02	41·61	0·04	8·39	0·15	49·42	99·6	91·3
92SZ-03	41·69	0·03	8·38	0·06	49·15	99·3	91·3
92SZ-04	41·45	0·04	9·60	0·14	48·55	99·8	90·0
92XL-01	41·44	0·04	9·74	0·09	48·10	99·4	89·8
92XL-02	41·67	0·07	7·95	0·13	49·54	99·4	91·7
92XL-04	41·35	0·01	10·29	0·12	47·84	99·6	89·2
1204-1-1	41·35	0·05	9·07	0·10	48·61	99·2	90·5
LTX-06	41·40	0·04	9·53	0·09	48·41	99·5	90·1
HPX-02	41·43	0·03	9·61	0·07	48·39	99·5	90·0
HPX-06	41·26	0·05	9·20	0·10	48·56	99·2	90·4
HPX-08	41·20	0·05	9·63	0·13	48·34	99·4	89·9

Fo %, forsterite content = Mg/(Mg + Fe) × 100 atomic ratio.

Table 3: Clinopyroxene trace element abundances (ICP-MS, ppm) in eastern China spinel-facies mantle xenoliths

	Hannuoba		Fansi		Linqu				Penglai			Qixia					Shangliao					Xuwen	Ninghai
Sample:	92HD-01	92HD-02	SF-20	SF-21	92LQ-01	92LQ-02	92LQ-04	92LQ-09	92PL-01	92PL-07	92PL-36	92QX-02	92QX-03	92QX-04	92QX-05	92QX-06	92SL-01	92SL-02	92SL-04	92SL-13	92SL-14	LTX-06	1204-1-1
Ti	1500	1239	1680	2113	2322	1825	2912	1159	3264	2672	2150	1407	2432	683	4115	250	2631	1566	1201	1929	955	2639	1511
Sr	14·7	35·1	39·7	168·8	54·2	54·1	31·0	274·8	65·3	69·5	33·6	240·0	365·5	131·8	121·8	98·9	69·1	101·5	60·3	122·3	35·6	87·0	31·6
Y	11·5	8·8	10·8	13·3	15·6	14·5	18·2	7·8	19·1	16·9	17·5	11·2	15·5	8·3	29·9	2·5	17·5	12·3	7·7	14·4	8·1	42·4	6·9
Zr	7·8	15·4	10·9	39·2	27·9	8·9	22·6	12·8	33·1	27·9	9·7	8·4	65·6	11·7	29·9	6·9	30·2	33·6	7·5	96·4	10·9	34·7	14·9
Hf	0·62	0·63	0·47	1·05	1·05	0·49	1·01	0·86	1·08	1·29	0·53	0·36	1·85	0·34	1·71	0·17	0·98	1·23	0·26	1·35	0·51	1·23	0·51
Nb	0·63	0·89	0·51	0·62	0·26	1·14	0·28	0·96	0·37	1·20	0·19	1·39	2·06	0·95	1·47	1·05	0·36	1·59	0·75	4·74	0·31	0·23	0·69
Ba	3·28	0·12	1·19	12·38	0·32	0·34	0·63	2·70	0·73	0·75	0·33	56·03	301·3	15·35	14·60	11·27	0·65	0·53	1·30	2·15	0·52	14·61	19·90
Th	0·16	0·11	0·06	0·79	0·03	0·15	0·02	0·65	0·04	0·38	0·02	0·15	0·57	0·07	0·48	0·16	0·02	0·59	0·18	0·51	0·01	0·08	0·12
La	0·49	1·02	1·26	5·73	0·62	1·74	0·23	6·57	0·77	1·30	0·26	1·29	20·38	1·89	0·44	2·37	0·71	3·68	2·60	4·48	0·17	24·01	1·10
Ce	1·10	2·48	3·13	13·85	3·13	3·32	1·36	22·40	3·11	3·63	1·29	2·49	63·78	4·86	1·58	4·96	2·42	10·07	4·92	12·18	0·85	32·36	3·10
Pr	0·25	0·41	0·51	1·81	0·72	0·46	0·40	3·79	0·62	0·60	0·30	0·34	9·97	0·68	0·43	0·63	0·44	1·72	0·66	1·85	0·20	5·95	0·53
Nd	1·72	2·20	2·59	7·76	4·48	2·39	2·94	17·60	3·94	3·60	2·16	1·72	46·45	2·86	3·20	2·59	2·69	7·76	3·00	8·42	1·28	24·39	2·92
Sm	0·82	0·83	0·85	1·92	1·73	1·12	1·57	3·64	1·62	1·44	1·20	0·81	9·42	0·58	2·11	0·53	1·33	2·01	0·98	2·19	0·68	6·29	0·99
Eu	0·38	0·35	0·34	0·71	0·69	0·49	0·62	0·98	0·70	0·63	0·52	0·39	2·49	0·22	0·96	0·16	0·61	0·71	0·39	0·88	0·28	2·11	0·41
Gd	1·47	1·19	1·26	2·30	2·28	1·74	2·49	3·07	2·51	2·27	2·03	1·47	7·02	0·72	3·83	0·44	2·20	2·01	1·28	2·75	1·03	6·82	1·40
Tb	0·29	0·21	0·26	0·42	0·41	0·33	0·45	0·33	0·45	0·43	0·44	0·26	0·81	0·13	0·82	0·07	0·43	0·38	0·21	0·45	0·20	1·20	0·21
Dy	2·13	1·61	1·90	2·50	2·88	2·57	3·30	1·93	3·38	3·12	3·07	1·95	3·88	1·22	5·70	0·44	3·04	2·23	1·46	2·90	1·51	7·18	1·34
Ho	0·46	0·34	0·43	0·51	0·61	0·58	0·66	0·32	0·70	0·65	0·68	0·45	0·63	0·30	1·24	0·11	0·68	0·55	0·33	0·60	0·34	1·38	0·27
Er	1·39	1·03	1·30	1·50	1·82	1·71	2·10	0·84	2·18	2·05	2·14	1·38	1·49	1·02	3·50	0·34	2·06	1·61	0·92	1·72	0·96	3·92	0·79
Tm	0·20	0·15	0·18	0·21	0·27	0·25	0·27	0·11	0·30	0·29	0·32	0·17	0·17	0·17	0·46	0·05	0·31	0·24	0·16	0·24	0·15	0·54	0·10
Yb	1·22	0·81	1·09	1·28	1·71	1·50	1·89	0·66	2·06	1·72	1·85	1·15	1·09	1·18	2·94	0·39	1·89	1·45	0·88	1·50	0·89	3·61	0·66
Lu	0·17	0·13	0·16	0·19	0·25	0·21	0·28	0·10	0·30	0·26	0·27	0·18	0·16	0·18	0·43	0·07	0·29	0·23	0·12	0·21	0·13	0·50	0·09

Table 3: continued

	Huinan					Yitong					Shangzhi				Xilong			Wenchang			Standard and blank			
Sample:	92HN-07	92HN-09	92HN-11	92HN-16	92HN-21	92YT-01	92YT-03	92YT-04	92YT-07	92YT-10	92SZ-01	92SZ-02	92SZ-03	92SZ-04	92XL-01	92XL-02	92XL-04	HPX-02	HPX-06	HPX-08	BHVO-1	BEN	NIMN	Blank
Ti	2033	2047	3686	2074	2463	1390	3002	350	2197	402	2343	705	3048	2890	2509	655	2954	1747	2138	671	15397	15092	1026	2·4
Sr	19·4	18·7	132·3	13·4	41·3	3·3	123·5	58·8	22·0	146·8	73·4	437·8	54·9	91·2	85·6	338·5	137·0	60·1	74·3	61·4	397·8	1494·5	260·1	0·10
Y	17·1	17·4	16·1	15·7	9·9	12·5	16·0	1·3	14·8	3·1	16·3	9·6	17·4	17·0	17·2	11·2	19·7	19·0	16·4	15·2	24·2	28·0	5·8	0·04
Zr	11·7	14·8	67·4	9·4	13·5	3·3	23·7	1·7	10·6	12·3	29·3	17·2	28·6	22·6	34·3	108·5	42·0	23·6	23·6	20·1	167·1	271·5	11·6	0·21
Hf	0·73	1·17	2·22	0·60	0·64	0·33	0·79	0·05	0·55	0·48	0·96	0·58	1·28	0·81	1·20	2·54	1·34	1·01	0·89	0·74	6·23	6·32	0·49	0·088
Nb	0·33	0·74	1·02	0·31	0·38	0·36	0·59	0·54	0·20	1·16	0·50	6·41	0·75	0·63	1·45	4·83	2·95	1·28	0·29	0·41	20·90	113·75	1·08	0·074
Ba	2·82	5·26	2·05	0·45	1·11	0·38	0·74	1·03	0·39	2·30	5·54	6·03	5·30	2·48	76·25	227·5	39·93	6·73	3·61	1·81	130·8	1063·1	82·9	0·300
Th	0·02	0·46	0·12	0·02	0·03	0·04	0·26	0·06	0·03	0·34	0·10	10·55	0·15	0·07	0·16	3·13	0·29	0·45	1·83	0·16	2·34	11·06	0·42	0·043
La	0·17	0·56	6·70	0·52	1·39	0·10	6·94	1·48	0·44	5·08	0·80	59·35	1·36	1·66	2·04	13·60	3·17	2·70	4·92	2·82	15·69	84·55	3·22	0·076
Ce	0·65	0·89	22·23	0·66	3·34	0·20	16·30	2·35	1·37	10·73	2·68	50·60	4·97	5·59	4·90	32·05	7·12	6·55	6·89	6·49	38·25	158·88	5·85	0·031
Pr	0·23	0·27	3·80	0·21	0·66	0·08	2·18	0·28	0·30	1·35	0·55	3·75	0·89	0·95	0·83	4·46	1·17	0·91	0·90	0·84	5·36	17·90	0·74	0·018
Nd	1·71	2·10	19·23	1·81	3·92	0·76	10·09	1·04	2·06	5·06	3·29	12·20	5·11	5·16	4·71	18·85	6·07	4·37	4·25	4·18	24·55	68·44	3·21	0·130
Sm	1·17	1·24	4·95	1·10	1·45	0·67	2·55	0·24	1·08	1·00	1·35	2·03	1·93	1·72	1·82	4·69	2·16	1·76	1·51	1·59	6·13	12·48	0·84	0·119
Eu	0·53	0·61	1·67	0·49	0·55	0·31	0·91	0·06	0·50	0·35	0·58	0·65	0·73	0·73	0·73	1·41	0·84	0·70	0·60	0·56	2·17	4·09	0·61	0·033
Gd	1·95	2·15	4·86	1·94	1·86	1·24	2·77	0·26	1·80	0·87	2·08	1·90	2·72	2·41	2·48	4·62	3·17	2·54	2·35	2·16	6·38	12·13	0·94	0·094
Tb	0·41	0·45	0·70	0·39	0·32	0·29	0·50	0·04	0·36	0·16	0·41	0·29	0·49	0·43	0·47	0·63	0·55	0·49	0·44	0·42	0·97	1·41	0·16	0·019
Dy	3·00	3·18	3·91	2·81	2·06	2·16	3·10	0·27	2·57	0·70	2·97	1·81	3·27	3·20	3·34	3·01	3·81	3·35	3·15	2·79	5·50	6·94	1·09	0·057
Ho	0·69	0·71	0·67	0·61	0·42	0·49	0·63	0·06	0·56	0·16	0·63	0·39	0·68	0·68	0·73	0·48	0·82	0·74	0·68	0·63	1·02	1·11	0·23	0·019
Er	2·09	2·10	1·73	1·97	1·16	1·45	1·83	0·15	1·72	0·38	1·92	1·10	1·96	2·08	2·08	1·13	2·43	2·13	2·00	1·83	2·59	2·72	0·69	0·062
Tm	0·31	0·32	0·19	0·28	0·16	0·22	0·26	0·02	0·26	0·05	0·28	0·16	0·27	0·30	0·28	0·13	0·33	0·32	0·28	0·26	0·36	0·33	0·10	0·018
Yb	1·85	1·85	1·22	1·69	0·98	1·37	1·48	0·13	1·59	0·34	1·77	0·98	1·63	1·88	1·88	0·78	2·10	1·92	1·85	1·63	2·08	1·90	0·65	0·072
Lu	0·27	0·27	0·16	0·25	0·13	0·19	0·21	0·02	0·21	0·05	0·26	0·15	0·26	0·30	0·27	0·12	0·30	0·28	0·26	0·23	0·32	0·26	0·10	0·018

Table 4: Representative Sr and Nd isotope compositions of clinopyroxenes in eastern China spinel-facies mantle xenoliths

Locality	Sample	$^{87}Sr/^{86}Sr$	$^{143}Nd/^{144}Nd$
On North China Craton			
Hannuoba	92HD-01	0·703038±3	0·513122±14
Hannuoba	92HD-02	0·703666±6	0·512783±31
Fansi	SF-20	0·704103±7	0·512726±28
Fansi	SF-21	0·705489±6	0·511909±31
Linqu	92LQ-01	0·703834±14	0·512863±25
Linqu	92LQ-02	0·703046±7	0·513032±32
Linqu	92LQ-04	0·702386±3	0·513615±16
Linqu	92LQ-09	0·703889±3	0·512869±26
Penglai	92PL-01	0·701845±4	0·514009±28
Penglai	92PL-07	0·703066±6	0·513169±23
Penglai	92PL-36	0·703303±6	0·513305±8
Qixia	92QX-02	0·703934±4	0·512801±28
Qixia	92QX-03	0·709560±5	0·511409±5
Qixia	92QX-04	0·703592±5	0·513039±15
Qixia	92QX-05	0·703962±6	0·512708±23
Qixia	92QX-06	0·704026±5	0·512334±28
Off-craton NE and SE China fold belts			
Shangliao	92SL-01	0·702231±6	n.d.
Shangliao	92SL-02	0·704915±7	0·512257±18
Shangliao	92SL-04	0·702465±6	n.d.
Shangliao	92SL-13	0·703481±7	0·512764±28
Shangliao	92SL-14	0·702839±7	n.d.
Huinan	92HN-07	0·703083±14	0·512714±28
Huinan	92HN-09	0·702437±21	n.d.
Huinan	92HN-11	0·705470±21	0·512686±13
Huinan	92HN-16	0·702624±9	n.d.
Huinan	92HN-21	0·703651±8	n.d.
Yitong	92YT-01	0·704222±21	0·513003±28
Yitong	92YT-03	0·704057±14	n.d.
Yitong	92YT-04	0·705073±21	0·512188±23
Yitong	92YT-07	0·702925±14	0·513256±13
Yitong	92YT-10	0·704334±14	0·512497±29
Shangzhi	92SZ-01	0·704506±28	n.d.
Shangzhi	92SZ-02	0·706186±25	0·512562±22
Shangzhi	92SZ-03	0·703595±21	0·513353±30
Shangzhi	92SZ-04	0·703094±28	0·513701±34
Xilong	92XL-01	0·702781±4	0·513263±11
Xilong	92XL-02	0·703666±4	0·512962±7
Xilong	92XL-04	0·702904±14	0·513162±27
Ninghai	1204-1-1	0·703606±7	0·513186±28
Xuwen	LTX-06	0·703046±12	n.d.
Wenchang	HPX-02	0·702241±12	0·513232±16
Wenchang	HPX-06	0·703359±13	n.d.
Wenchang	HPX-08	0·702510±12	0·513376±5

n.d., not detected.

ocean basins or tectonically active continents where spinel-facies lherzolites predominate (e.g. Stosch & Seck, 1980; Hauri *et al.*, 1993; Sen *et al.*, 1993).

Olivine and orthopyroxene modes and chemistry

Electron microprobe studies indicate that olivines in the eastern China xenoliths are basically homogeneous with no significant intra-grain and inter-grain variations. In terms of forsterite content, the maximum discrepancy between five analyses, within a single grain or between five discrete grains, is <0·4%. The olivine data (Table 2) represent average compositions of five analyses and their NiO content correlates with magnesium content. Olivine websterites have a much wider compositional range than the spinel lherzolites, especially in on-craton localities. Of the three samples studied, one from Hannuoba (92HD-02) has the highest MgO content (49·8%) and the highest NiO (0·6%) content of all the 'on-craton' xenoliths. Another from Qixia (92QX-03) has an extremely high iron content (FeO = 16%) and the lowest NiO (0·06%). On and off the craton, the olivines are similar in composition [$(MgO)_{on\text{-}craton}$ >48 wt % and $(MgO)_{off\text{-}craton}$ >46 wt %] (Fig. 3).

Orthopyroxene modal and olivine compositional data from on and off the North China Craton (Fig. 3a) are compared with data from other cratons and modern ocean basins (Fig. 3d). On-craton peridotites from Kaapvaal, South Africa (Fig. 3b) have a greater content of orthopyroxene than on-craton peridotites from Wiedemann Fjord–Ubekendt Island, Greenland, Tanzania and Lac de Gras, Canada (Fig. 3b) (Kelemen *et al.*, 1998; Griffin *et al.*, 1999*a*, 1999*b*; Lee & Rudnick, 2000). Except for a few scattered points, the combined cratonic datasets define a broad band of data with variable orthopyroxene mode and variable olivine composition. In the case of eastern China (Fig. 3a) both on- and off-craton spinel-facies peridotites have a modal orthopyroxene content similar to on-craton peridotites but the coexisting olivine is more iron rich. As such, the peridotites from eastern China are distinct from those found within the cratons of Canada, Greenland, Siberia, South Africa and Tanzania. However, the eastern China dataset occupies a similar field to high-temperature off-craton peridotites from South Africa (Boyd, 1989) (Fig. 3c), peridotites from tectonically active continents and peridotites from ocean basins (Fig. 3d). The important exception in any comparison of Chinese xenoliths with ocean basins is that peridotites from arc environments contain a high modal amount of magnesian olivines and as such are different. Indeed, several researchers have argued for a two-stage evolutionary process (e.g. Cox *et al.*, 1987) in the formation

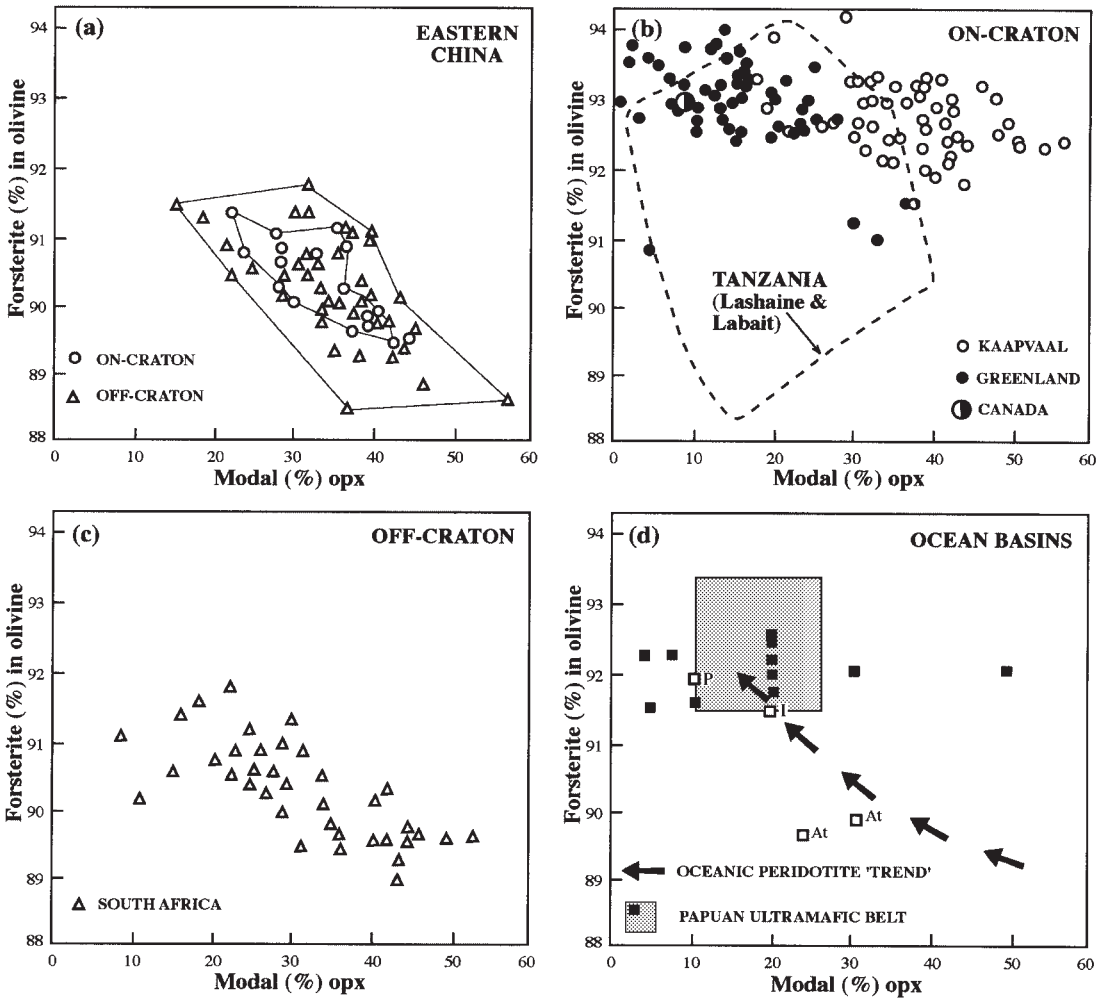

Fig. 3. Forsterite content vs modal abundance of orthopyroxene in mantle peridotites. (a) On- and off-craton spinel peridotitic xenoliths from eastern China plot as overlapping fields. (b) Garnet- and spinel-facies peridotites from cratons in Africa, Greenland and Canada (Boyd, 1989; Kelemen *et al.*, 1998; Lee & Rudnick, 2000) display a greater range in olivine composition and modal abundance. Kaapvaal peridotites are orthopyroxene rich and contain magnesian olivines whereas those from Greenland and Canada are more orthopyroxene poor. The garnet and spinel peridotites from the Tanzanian craton have a greater spread in olivine compositional data and orthopyroxene mode than other cratons. (c) South African off-craton peridotites are different from on-craton peridotites (Boyd, 1989) but they overlap with on-craton peridotites from Tanzania (Lee & Rudnick, 2000) and Greenland (Kelemen *et al.*, 1998). More importantly, off-craton peridotites from southern Africa are similar to on- and off-craton spinel peridotites from eastern China. (d) Spinel- and plagioclase-facies peridotites from the world's ocean basins and ophiolites [i.e. abyssal peridotites, ophiolitic metamorphic peridotites and orogenic (non-ophiolitic) peridotites] have a compositional range that can be represented as an oceanic peridotite 'trend' (Boyd, 1989). ■, arc-peridotites from the Papuan ultramafic belt [Kelemen *et al.*, (1998) and references therein]. (Note the similarity between the eastern China dataset and oceanic peridotites from the Atlantic and Indian Oceans.) P, Pacific Ocean; I, Indian Ocean; At, Atlantic Ocean [after Menzies (1991) and references therein].

of cratonic peridotites. Melt-rock reaction in arc environments has been recently invoked (Rudnick *et al.*, 1994; Kelemen *et al.*, 1998) as an explanation for the highly magnesian nature of cratonic peridotites. The Chinese peridotites are more similar to peridotites found in off-craton localities or peridotites from ocean basins than they are to low-temperature cratonic peridotites that lie on a shield geotherm.

Clinopyroxene trace element geochemistry

Trace element abundances in clinopyroxenes from eastern China spinel-facies mantle xenoliths are given in Table 3 and plotted in Fig. 4. Clinopyroxenes from on- and off-craton peridotites display the same overall variation in chondrite-normalized rare earth element (REE) pattern from light REE (LREE)-depleted compositions, through transitional LREE profiles to

LREE-enriched profiles (Fig. 4). In turn, these groups are subdivided into moderate to strong depletions in the LREE, irregular or flat REE profile and moderate to strong enrichments in the LREE (Fig. 4).

Moderately LREE-depleted clinopyroxenes from on- and off-craton localities have almost identical middle REE (MREE), heavy REE (HREE) and Y concentrations ($\sim 10 \times$ C1 chondrites) and display no REE fractionation from Eu to Lu. Strongly LREE-depleted clinopyroxenes display a slightly greater range in MREE and HREE but the HREE remain around $10 \times$ C1 chondrites. These pyroxenes are similar to LREE-depleted pyroxenes (i.e. Type 1A) found in peridotites world-wide (McDonough & Frey, 1989) and there does not appear to be any systematic difference between on- and off-craton peridotites. Clinopyroxenes with irregular and flat chondrite-normalized REE profiles have a very restricted REE abundance between $4 \times$ and $20 \times$ C1 chondrite and show no significant LREE–HREE fractionation (Fig. 4). LREE-enriched clinopyroxenes show a considerable range in Ce/Yb very different from the other two groupings. Clinopyroxenes with an enrichment in the LREE have been reported from many other localities (e.g. Stosch & Seck, 1980; Johnson *et al.*, 1990; Sen *et al.*, 1993) but for eastern China there appear to be no systematic differences between on- and off-craton clinopyroxenes.

The style of LREE enrichment observed in clinopyroxenes from on-craton xenoliths in eastern China is more akin to that observed in spinel-facies basalt-hosted xenoliths from around the world and very different from on-craton garnet-facies kimberlite-hosted xenoliths from around the world [Menzies *et al.* (1987) and references therein]. Kimberlite-hosted cratonic peridotites contain clinopyroxenes with marked depletions in the HREE ($<1 \times$ chondrite) relative to the LREE ($>10 \times$ chondrite) with the exception of deformed, high-temperature peridotites. In contrast, clinopyroxenes from off-craton kimberlite- and basalt-hosted peridotites display a range in REE characteristics that includes LREE-depleted and LREE-enriched clinopyroxenes. Furthermore, clinopyroxene data from ancient and modern oceanic peridotites are dominated by LREE-depleted clinopyroxenes (e.g. Johnson *et al.*, 1990) similar to the 'strongly LREE-depleted' pyroxenes from eastern China (Fig. 4). Also, orogenic–ophiolitic lherzolites contain pyroxenes with LREE-depleted profiles at $\sim 1 \times$ chondrite-normalized LREE abundances and $\sim 10 \times$ chondrite-normalized HREE abundances (e.g. Bodinier *et al.*, 1991). These compare favourably with the 'moderately LREE-depleted' and 'strongly LREE-depleted' pyroxenes from eastern China (Fig. 4).

Clinopyroxenes from off- and on-craton xenoliths in eastern China (Type I and II) display similar Sr abundances but a much larger variation in Th [Sr = 3–438 ppm; $(Th)_N$ = 0·2–360; Table 3] relative to kimberlite-hosted on-craton xenoliths [Sr = 15–400 ppm; $(Th)_N$ = 0·6–27ppm]. The abundance of Sr and Th in off-craton clinopyroxenes correlates with the LREE [Nd vs Sr; $(Ce/Yb)_N$ vs $(Sr)_N$ or $(Th)_N$]. Strongly LREE-depleted and extremely LREE-enriched pyroxenes from off-craton localities have a range in Sr/Nd ratio whereas most xenoliths from on-craton localities have a near-constant Sr/Nd ratio of 15 ± 5, similar to the chondritic ratio (McDonough & McCulloch, 1987). Some samples with Sr enrichment relative to Nd also have rather irregular REE profiles.

Sr and Nd isotopes in clinopyroxenes

Representative Sr and Nd isotope ratios in clinopyroxenes from eastern China spinel-facies mantle xenoliths are given in Table 4 and shown in Fig. 5. Apart from one sample, clinopyroxenes from on-craton localities in eastern China (Fig. 5a) are characterized by a similar range in Sr and Nd isotopes to off-craton localities. Compared with on-craton xenoliths from eastern China, a greater range in $^{87}Sr/^{86}Sr$ and $^{143}Nd/^{144}Nd$ ratios is observed in other on-craton xenoliths. The on- and off-craton basalt-hosted xenoliths from eastern China have greater similarities with off-craton xenoliths from around the world and with oceanic peridotites (Fig. 5c). The latter are characterized by a restricted range in Sr and Nd isotopes with the majority of samples located in the top left-hand quadrant, a location consistent with a history of melt extraction. Some clinopyroxenes from eastern China have Sr and Nd isotopic affinities to on-craton peridotites from elsewhere. The bulk of the isotope data points to an affinity with off-craton–oceanic processes as did the modal mineralogy of the eastern China peridotites.

DISCUSSION

Pioneering work by Zhou & Armstrong (1982) indicated that the Cenozoic lithospheric mantle beneath eastern China was laterally and vertically heterogeneous, a conclusion supported by later work (e.g. Zhou & Zhu, 1992). Cenozoic basalts from eastern China were shown to have isotopic characteristics similar to those of oceanic volcanic rocks and continental rift basalts, with the highest $^{87}Sr/^{86}Sr$ ratios occurring at Wudalianchi. These isotopic ratios, as well as incompatible trace elements in Cenozoic alkali basalts, required an 'enriched' component in their mantle source and it was proposed by several workers that this enriched source was shallow and located within the sub-lithospheric mantle (Zhang *et al.*, 1991, 1995, 1998; Zhou & Zhu, 1992). The xenolith data presented

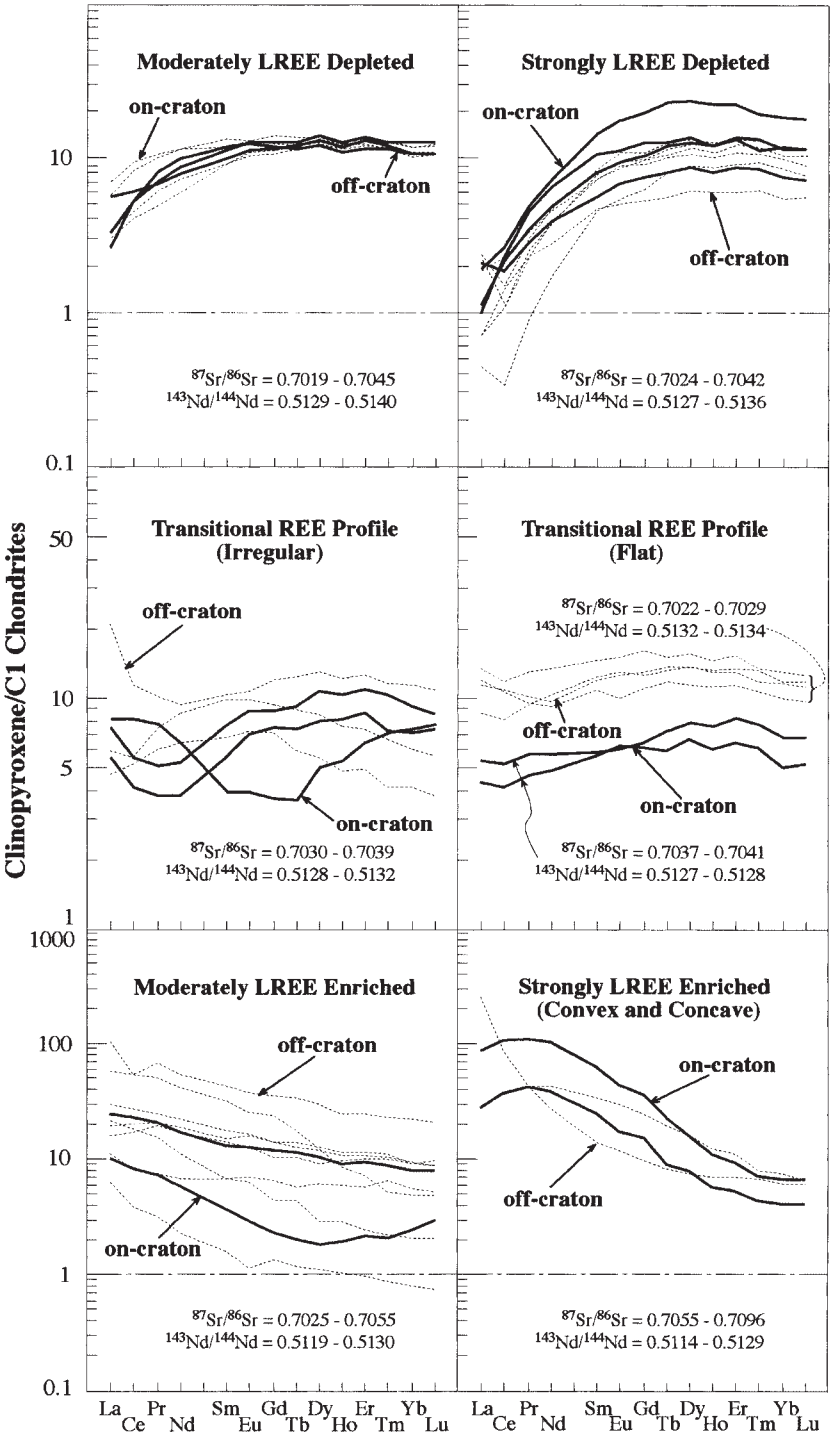

Fig. 4. Chondrite-normalized REE patterns of clinopyroxenes separated from the spinel-facies peridotites in on-craton (continuous lines) and off-craton (dashed lines) localities, eastern China. It should be noted that there is a large variation in REE patterns from extremely depleted to strongly enriched in the LREE. Also, no systematic difference exists between on- and off-craton localities in eastern China, which contrasts with the REE characteristics of clinopyroxenes from on- and off-craton localities elsewhere in the world (e.g. McDonough & Frey, 1989). Chondrite values are from Anders & Grevesse (1989).

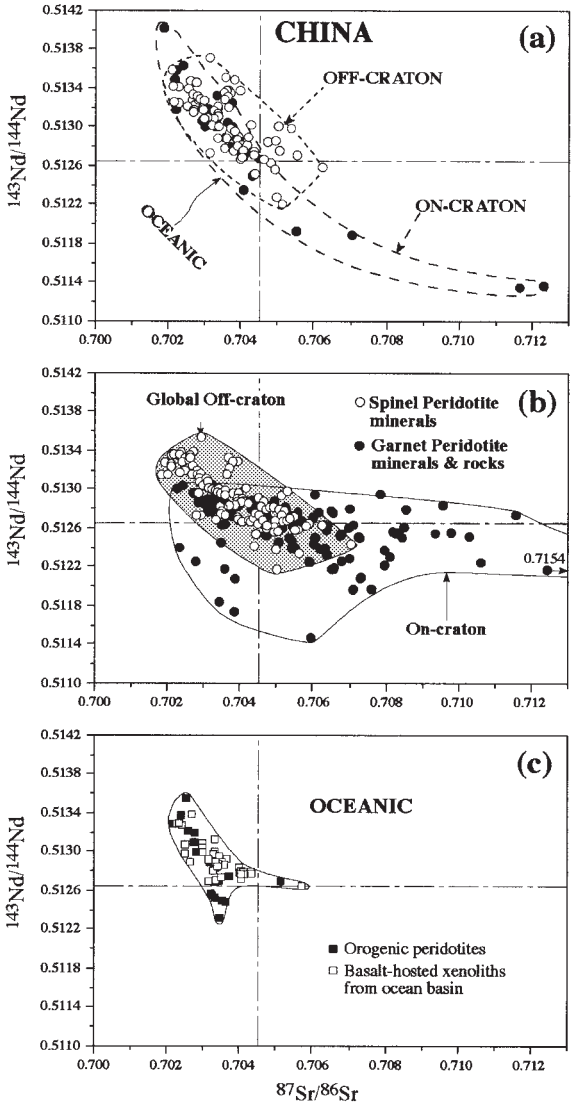

Fig. 5. Sr and Nd isotope variation in mantle peridotites and their constituent minerals. (a) The peridotite and pyroxenite data reported in Table 4 primarily plot in the top left-hand quadrant (depleted source regions) with two pyroxenites from Fansi and Qixia plotting in the lower right-hand quadrant in a similar location to the pyroxenite and megacryst data of Tatsumoto *et al.* (1992) and W. M. Fan (unpublished data, 1999). These data are not necessarily evidence for enriched mantle because the petrogenesis of pyroxenites and megacrysts may involve crustal rocks and/or lower-crustal processes. Other data sources include Song & Frey (1989), Deng & MacDougall (1992), Qi *et al.* (1995) and X. Xu *et al.* (1998). (b) Peridotite xenoliths from other on- and off-craton locations around the world (Menzies & Murthy, 1980; Kramers *et al.*, 1981, 1983; Richardson *et al.*, 1985, 1993; Erlank *et al.*, 1987; Walker *et al.*, 1989; Hawkesworth *et al.*, 1990; Pearson *et al.*, 1995*a*). It should be noted that even more extreme on-craton mantle heterogeneity (i.e. high Sr and low Nd isotope ratios) was reported by Cohen *et al.* (1984; Tanzanian craton), Menzies & Halliday (1988; North Atlantic craton) and Carlson & Irving (1994; Wyoming craton). (c) Oceanic peridotites include orogenic and xenolithic peridotites [Menzies (1991) and references therein].

in this study indicate that in tectonically active eastern China there is an overall lack of enriched reservoirs, much of the sub-Moho lithosphere beneath eastern China being chemically and isotopically depleted.

Basalt-hosted spinel peridotites from eastern China have similarities to shallow mantle occurring beneath tectonically active continents (e.g. Basin and Range) or modern ocean basins. The similarities include: a predominance of mantle peridotites that formed in the spinel lherzolite stability field; an olivine:clinopyroxene: orthopyroxene mode that is similar to that found beneath tectonically active continents or the lower oceanic lithosphere; a forsterite content like that found in off-craton peridotites or in abyssal, ophiolitic and orogenic peridotites; and an 'oceanic' partial-melting trend commensurate with the modal variation in residual peridotites formed by extraction of basaltic melts from a primordial mantle source.

The broad similarities with an 'oceanic' provenance, despite the age of the overlying crust (i.e. 3·3 Ga), must argue for petrogenetic processes beneath the NCC similar to those that led to accretion of lower lithosphere beneath ocean basins and tectonically active continents. Several independent sources of information support the presence of relatively thin (spinel facies <75 km) lithosphere beneath eastern China. These include seismic, heat flow and thermobarometric data. Seismic tomography (Chen *et al.*, 1991; Polet & Anderson, 1995) indicates that the present-day lithosphere beneath eastern China is <100 km thick and may be ~80 km thick, with greatly thinned on-craton lithosphere around the Bohai Sea. Heat flow studies in eastern China (Teng *et al.*, 1983) support the presence of thin lithosphere and a shallow low-velocity structure similar to an ocean ridge. Indeed, a region of very high heat flow exists on the NCC in the vicinity of the Bohai Sea and Beijing (Fig 1). The measured heat flow corresponds to geotherms observed in tectonically active continents or ocean basins (50–105 mW/m^2). The eastern China geotherm, reconstructed from the geothermobarometry of garnet lherzolites, garnet websterites and spinel lherzolites, has a high thermal gradient similar to that of ocean basins or tectonically active continental regions such as SE Australia (Griffin *et al.*, 1998; X. Xu *et al.*, 1998).

Elemental and isotopic data for Chinese mantle xenoliths provide the most direct evidence for the degree of mantle heterogeneity. It is not known, however, to what extent the mantle sampled by spinel-facies xenoliths is related, in time and space, to that involved in the genesis of the volcanic rocks. Mantle xenoliths from eastern China have a magnesium-rich character (Fo >89) with minor iron-rich samples (Fo <89, Table 2). Their REE profiles vary from strongly REE depleted (Fig. 4) to extremely REE enriched. This may point to modification

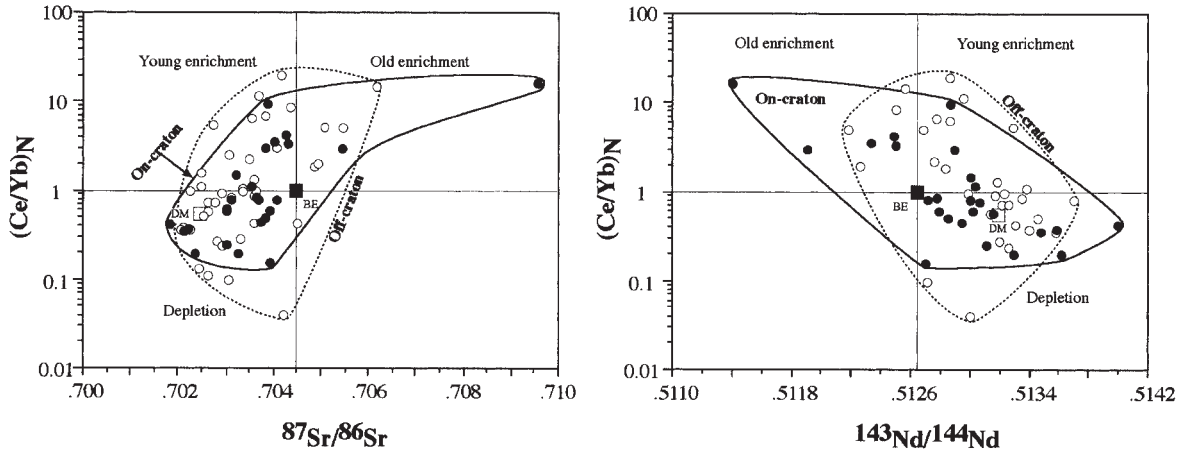

Fig. 6. $(Ce/Yb)_N$ vs Sr and Nd isotope ratios in clinopyroxenes from on- and off-craton spinel-facies mantle xenoliths. On- and off-craton data have the same elemental and isotopic characteristics with the exception of a few data points. Peridotite xenoliths from eastern China appear to have formed as a result of depletion processes. Data sources: Song & Frey (1989); Qi *et al.* (1995); Y.-G. Xu *et al.* (1998). BE and DM represent bulk earth and depleted MORB mantle, respectively.

of a protolith (LREE depleted) by a melt (LREE enriched). High field strength element (HFSE) and large ion lithophile element (LILE) heterogeneity is also apparent, as is a large range in Sr and Nd isotopic composition (Figs 5 and 6). Eastern China peridotites have a range in isotopes from a depleted mantle composition (i.e. $^{87}Sr/^{86}Sr = 0{\cdot}7035$, $^{143}Nd/^{144}Nd = 0{\cdot}5135$) toward an enriched mantle composition ($^{87}Sr/^{86}Sr > 0{\cdot}7045$, $^{143}Nd/^{144}Nd < 0{\cdot}5122$) (Fig. 5). Such an isotopic range straddles that observed in modern ocean basins and tectonically active continental regions with some of the characteristics of on-craton peridotites. Within a single locality such as Qixia and Shangliao, xenoliths exhibit variable REE profiles from extremely LREE depleted to LREE enriched (Table 3) as well as other trace elements, and single localities also exhibit large variations in Sr and Nd isotopes (Table 4). The variations in olivine composition, $(Ce/Yb)_N$ ratio and Sr–Nd isotopes for mantle xenoliths from different localities, and within single localities, demonstrate that the lithospheric mantle beneath the NCC and the NE China fold belts is locally and regionally heterogeneous (see Zhou & Armstrong, 1982).

Mantle history

Several aspects of the eastern China xenoliths indicate a role for partial melting processes in their origin. The magnesium-rich nature (Fo = 89·4–91·3%) in the dominant mineral, olivine, as well as a broadly positive correlation between MgO and NiO, suggests that the peridotites may represent the refractory residues formed by melt extraction (e.g. McDonough, 1990). The Chinese 'on-craton' xenoliths are petrographically distinct from the Kaapvaal 'on-craton' xenoliths, particularly with regard to their cpx/opx ratio (Fig. 2) and forsterite content (Fig. 3). Both on-craton and off-craton xenoliths from eastern China plot within the field of off-craton xenoliths from Kaapvaal or the field occupied by oceanic, abyssal or ophiolitic peridotites. One can argue that they have an 'oceanic' affinity. This indicates that the lithosphere beneath the NCC contrasts with typical continental lithospheric mantle beneath cratons such as Kaapvaal. The similarity with oceanic lithosphere, accreted at ridges by the extraction of basaltic melt from the asthenosphere, may indicate that recent accretion of mantle produced part of the lithospheric mantle during periods of Cenozoic volcanism. However, the existence of relatively undifferentiated garnet lherzolites from Mingxi may indicate that undifferentiated asthenosphere may be part of that accretionary process.

The depleted chondrite-normalized REE profiles of the spinel lherzolites from eastern China are similar to those of depleted mantle rocks occurring elsewhere as spinel-facies peridotites [e.g. abyssal peridotites, ophiolitic metamorphic peridotites, orogenic (non-ophiolitic) metamorphic peridotites and spinel-facies basalt-hosted xenoliths] (Fig. 4). Such peridotites are believed to have been involved in melt extraction (and transfer) processes at relatively shallow depths (i.e. ~75–80 km) in the absence of garnet. Melt transfer preferentially removes the LREE and Rb. When integrated over geological time, such elemental changes are recorded as low Sr and high Nd isotopic ratios (Fig. 5). This is consistent with the presence of depleted Sr and Nd isotopes in xenoliths from the NCC. The very low $^{143}Nd/^{144}Nd$ ratios and high $^{87}Sr/^{86}Sr$ ratios for several peridotites from Penglai,

Linqu and Hannuoba reveal a mantle component perhaps isolated from the convecting upper mantle for billions of years. Such material has not been reported from modern ocean basins and is more commonly reported from on-craton regions. However, in the case of eastern China, it occurs both on and off the craton and, as such, cannot be used as a unique piece of evidence for the presence of ancient lithosphere.

Some mantle rocks from eastern China show an enrichment in LREE and LILE (Fig. 4) that is inconsistent with them being a simple melt residue. Thus melt ingress or metasomatic enrichment is invoked and is best illustrated by the existence of very rare hydrous minerals in spinel lherzolites and/or pyroxenites (Tatsumoto *et al.*, 1992; Zhou & Zhu, 1992). In addition, the presence of irregular chondrite-normalized REE profiles (Fig. 4) illustrates processes that relate to melt migration (X. Xu *et al.*, 1998). One important aspect is that the LREE-enriched samples have a lower abundance of the HREE than the LREE-depleted samples. Clearly, the diversity of the REE patterns (Fig. 4) in clinopyroxenes from eastern China requires more than one enrichment mechanism. For example, the spoon-shaped patterns in clinopyroxenes from peridotites can be best accounted for by chromatographic metasomatism. For our database, we prefer a percolation-reaction model, which takes into account both chromatographic and melt-rock reaction effects and shows some similarities between the modelled REE patterns and the measured REE profiles [X. Xu *et al.* (1998) and references therein]. The spoon-shaped REE pattern is believed to be the product of very early stages of small-volume melt infiltration where percolation-controlled metasomatism was terminated as a result of incorporation into basaltic magma. The enrichment of La and Ce in small-volume melts leads to their enrichment in clinopyroxene relative to other LREE (Pr, Nd, Sm). On the other hand, the convex profile, apparent in strongly LREE-enriched samples, may reflect metasomatic recrystallization of previous clinopyroxene or direct crystallization from melts in a closed system. The latter suggestion is supported by the extremely high LREE in clinopyroxene and the iron content of olivine from an on-craton websterite.

The relationship between trace elements and isotopes is presented in Fig. 6. Most of the Chinese xenoliths are isotopically depleted but many of these depleted xenoliths are LREE enriched (Figs 5 and 6). This indicates 'recent' decoupling of trace elements and Nd isotopes as a result of addition of the LREE by a fluid. In contrast to such 'young' processes that may relate to the periods of volcanism there is an indication of possibly 'older' enrichments in the mantle. A few LREE-enriched xenoliths, mainly pyroxenites or megacrysts, have high $^{87}Sr/^{86}Sr$ and low $^{143}Nd/^{144}Nd$ ratios, which indicate a coupling of trace elements and isotopes that may reflect the presence of 'old' enrichment processes in the lithosphere (e.g. >2·5 Ga). However, as their origin is so complex the 'enriched' signature may also indicate input from crustal reservoirs.

Some insights into what type of melts may have been responsible for changes to the post-Archaean lithosphere are forthcoming from the application of published partition coefficient data to trace element data. Clinopyroxenes with convex REE profiles may be the products of equilibration with LREE-depleted silicate or non-silicate melts, or the products of direct crystallization from such LREE-depleted melts. These hypothetical melts are distinctly different from the compositions of oceanic island and mid-ocean ridge basalts. This indicates that the host alkaline silicate melts were not the melts that produced the trace element enrichment in these mantle xenoliths, a suggestion supported by isotope data. The large isotope variation in the mantle xenoliths is very different from the restricted range of isotopes in the host basalts. Partition coefficient data for clinopyroxene–carbonatite melts (Green *et al.*, 1992) permits the calculation of coexisting hypothetical equilibrium melts for LREE-enriched clinopyroxenes. This reveals a melt with elemental characteristics similar to those of natural carbonatites (Nelson *et al.*, 1988), which could account for the nature of the enriched xenoliths. It is very difficult to infer the composition of a hypothetical coexisting melt on the basis of trace elements in clinopyroxene without trace element data on coexisting minerals. We are certain that the metasomatic melt responsible for the trace element enrichment in some of these mantle xenoliths was LREE rich and Fe poor. The extent of the enrichment or depletion of Ti and Zr in such melts relative to the LREE is less certain and awaits more detailed study of the trace element geochemistry of coexisting phases.

CONCLUSIONS

The petrological and geochemical data presented in this paper allow us to answer the questions posed in the Introduction.

What is the nature of the sub-Moho mantle beneath eastern China?

Sub-crustal peridotites from eastern China are predominantly shallow-facies mantle rocks (i.e. spinel-facies 75–80 km). Their lherzolitic nature, olivine/orthopyroxene mode and the composition of olivine reveals remarkable similarities to the lithosphere found beneath tectonically active continents or modern ocean basins ($\sim$200 Ma).

Does on- and off-craton provinciality exist as it does in other parts of the world?

On- and off-craton provinciality is not clearly defined in eastern China. Although a small number of megacrysts and pyroxenites from the NCC have enriched Sr and Nd isotopes like on-craton peridotites from Kaapvaal, the majority of peridotites on and off the NCC are depleted in Sr and Nd isotopes.

What processes best account for the formation of lithospheric mantle beneath eastern China?

Most of the on- and off-craton peridotites from eastern China have evolved in response to processes similar to those responsible for the formation of the lower lithosphere in ocean basins or tectonically active continents. These processes are thought to relate to the extraction of basaltic magmas from the asthenosphere (~1300°C) with subsequent incorporation and accretion of residual peridotites. It is proposed that the spinel-facies peridotites represent shallow accretion of mantle during asthenospheric upwelling in the Phanerozoic.

How does present-day lithosphere compare with the Archaean lithosphere known to have survived until the Ordovician?

According to kimberlite-hosted xenolith data from the NCC, Ordovician lithosphere had an architecture similar to that of Archaean lithosphere. It was stable to garnet- and diamond-facies, cold (shield geotherm) and it reached a thickness of ~180–200 km. This is in marked contrast to Cenozoic lithosphere, which is 'oceanic' with some indication of an 'older' pre-existent lithosphere. It has been proposed that the Archaean lithospheric keel was affected by thermo-tectonic processes (Menzies *et al.*, 1993; Griffin *et al.*, 1998) in the form of plume activity, delamination or rifting, or a combination of such processes.

ACKNOWLEDGEMENTS

The late Keith Cox was an inspiration to us all, a great companion in the field or on a long plane flight. He will never be forgotten for his friendship, his support, his dry wit and those memorable 'stories'. Keith always believed that we should understand the petrology and mineralogy of our rocks before tackling geochemistry, particularly isotopes.

The Royal Society and the Chinese Academy of Sciences are thanked for supporting a link with Changsha University (Dr Fan Weiming), the catalyst for this project. The Overseas Research Student Scheme (UK) and the K. C. Wong Education Foundation (Hong Kong) are thanked for financial support in a form of a pre-doctoral year and a 3-year doctoral studentship to Hongfu Zhang (Northwestern–Beijing) tenable at Royal Holloway College, University of London. Andy Beard is thanked for his technical assistance with electron microprobe and Sr–Nd isotope analyses. The authors appreciate the considerable efforts of Graham Pearson, both as a doctoral examiner of H.Z. and as a reviewer. The detailed and constructive comments of Roberta Rudnick have tightened up this manuscript considerably. Roberta is thanked for her time and effort.

This study was supported by grants from the Chinese Academy of Sciences (KZ951-A1-401-01) and from the National Sciences Foundation of China (49733110).

REFERENCES

Anders, E. & Grevesse, N. (1989). Abundances of the elements: meteoritic and solar. *Geochimica et Cosmochimica Acta* **53**, 197–214.

Anderson, D. L., Tanimoto, T. & Zhang, Y. (1992). Plate tectonics and hotspots: the third dimension. *Science* **256**, 1645–1650.

Bodinier, J. L., Menzies, M. A. & Thirlwall, M. F. (1991). Elemental and isotopic geochemistry of the Lanzo lherzolite massif—implications for the temporal evolution of the MORB source. *Journal of Petrology* **6**, 27–42.

Boyd, F. R. (1989). Compositional distinction between oceanic and cratonic lithosphere. *Earth and Planetary Science Letters* **96**, 15–26.

Boyd, F. R. & Nixon, P. H. (1978). Ultramafic nodules from the Kimberley pipes, South Africa. *Geochimica et Cosmochimica Acta* **42**, 1367–1382.

Boyd, F. R., Gurney, J. J. & Richardson, S. H. (1985). Evidence for a 150–200 km thick Archaean lithosphere from diamond inclusion thermobarometry. *Nature* **315**, 387–389.

Boyd, F. R., Pokhilenko, N. P., Pearson, D. G., Mertzman, S. A., Sobolev, N. V. & Finger, L. W. (1997). Composition of the Siberian cratonic mantle: evidence from Udachnaya peridotite xenoliths. *Contributions to Mineralogy and Petrology* **128**, 228–246.

Carlson, R. W. & Irving, A. J. (1994). Depletion and enrichment history of subcontinental lithospheric mantle: an Os, Sr, Nd and Pb isotopic study of ultramafic xenoliths from the northwestern Wyoming Craton. *Earth and Planetary Science Letters* **126**, 457–472.

Carswell, D. A. & Dawson, J. B. (1970). Garnet peridotite xenoliths in South Africa kimberlite pipes and their petrogenesis. *Contributions to Mineralogy and Petrology* **25**, 163–184.

Chen, J. (1971). Petrology and chemistry of garnet lherzolite nodules in kimberlite from South Africa. *American Mineralogist* **56**, 2098–2110.

Chen, G. Y., Song, Z.-H., An, C.-Q., Cheng, L.-H., Zuang, Z., Fu, Z.-W., Lu, Z.-L. & Hu, J.-F. (1991). Three dimensional crust and upper mantle structure of the North China region. *Acta Geophysica Sinica* **34**, 172–181.

Chi, J. S., Lu, F. X., Zhao, L., Zhao, Z. H., Zheng, J. P. & Deng, J. F. (1992). *A Study of Primary Diamond Deposits North-China Craton: Genesis and Prospects*. Beijing: China University of Geoscience, 355 pp. (in Chinese).

Cohen, R. S., O'Nions, R. K. & Dawson, J. B. (1984). Isotope geochemistry of xenoliths from East Africa: implications for development of mantle reservoirs and their interaction. *Earth and Planetary Science Letters* **68**, 209–220.

Cox, K. G., Gurney, J. & Harte, B. (1973). Xenoliths from the Matsoku pipe. In: Nixon, P. H. (ed.) *Lesotho Kimberlites*. Cape Town: National Development Corporation, pp. 76–100.

Cox, K. G., Smith, M. R. & Beswetherick, S. (1987). Textural studies of garnet lherzolites: evidence of exsolution origin from high-temperature harzburgites. In: Nixon, P. H. (ed.) *Mantle Xenoliths*. New York: John Wiley, pp. 537–551.

Dawson, J. B. (1980). *Kimberlites and their Xenoliths*. Berlin: Springer, 252 pp.

Deng, F. L. & Macdougall, J. D. (1992). Proterozoic depletion of the lithosphere recorded in mantle xenoliths from Inner Mongolia. *Nature* **360**, 333–336.

Dick, H. J. B. & Fisher, R. L. (1984). Mineralogic studies of the residues of mantle melting: abyssal and alpine-type peridotites. In: Kornprobst, J. (ed.) *Kimberlites II: The Mantle and Crust–Mantle Relationships. Proceedings of the 3rd International Kimberlite Conference, 2*. Amsterdam: Elsevier, pp. 295–308.

Erlank, A. J., Waters, F. G., Hawkesworth, C. J., Haggerty, S. E., Allsopp, H. L., Rickard, R. S. & Menzies, M. A. (1987). Evidence for mantle metasomatism in peridotite nodules from the Kimberley Pipes, South Africa. In: Menzies, M. A. & Hawkesworth, C. J. (eds) *Mantle Metasomatism*. London: Academic Press, pp. 221–311.

Fan, Q. & Hooper, P. R. (1991). The Cenozoic basaltic rocks of Eastern China: petrology and chemical composition. *Journal of Petrology* **32**, 765–810.

Grand, S. P. (1994). Mantle shear structure beneath the Americas and surrounding oceans. *Journal of Geophysical Research* **99**, 11591–11621.

Green, D. H., Hibberson, W. O. & Jaques, A. L. (1979). Petrogenesis of mid-ocean ridge basalts. In: McElhinney, M. W. (ed.) *The Earth: its Origin, Structure and Evolution*. London: Academic Press, pp. 265–299.

Green, T. H., Adam, J. & Sie, S. H. (1992). Trace element partitioning between silicate minerals and carbonatite at 25 kbar and application to mantle metasomatism. *Mineralogy and Petrology* **46**, 179–184.

Griffin, W. L., Kaminsky, F. V. K., Ryan, C. G., O'Reilly, S. Y., Win, T. T. & Ilupin, I. P. (1996). Thermal state and composition of the lithospheric mantle beneath Daldyn kimberlite field, Yakutia. *Tectonophysics* **262**, 19–33.

Griffin, W. L., Zhang, A., O'Reilly, S. Y. & Ryan, C. G. (1998). Phanerozoic evolution of the lithosphere beneath the Sino-Korean craton. In: Flower, M. F. J., Chung, S.-L., Lo, C.-H. & Lee, T. Y. (eds) *Mantle Dynamics and Plate Interactions in East Asia, Geophysical Monograph, American Geophysical Union* **27**, 107–126.

Griffin, W. L., Doyle, B. J., Ryan, C. G., Pearson, N. J., O'Reilly, S. Y., Davies, R., Kivi, K., Van Achterbergh, E. & Natapov, L. M. (1999*a*). Layered mantle lithosphere in the Lac de Gras area, Slave Craton: composition, structure and origin. *Journal of Petrology* **40**, 705–728.

Griffin, W. L., Fisher, N. I., Friedman, J., Ryan, C. G. & O'Reilly, S. Y. (1999*b*). Cr-pyrope garnets in the lithospheric mantle 1. Compositional systematics and relations to tectonic setting. *Journal of Petrology* **40**, 679–704.

Hanson, G. N. & Langmuir, C. H. (1978). Modelling of major elements in mantle-melt systems using trace element approaches. *Geochimica et Cosmochimica Acta* **42**, 725–741.

Hauri, E. H., Shimizu, N., Dieu, J. J. & Hart, S. R. (1993). Evidence for hotspot-related carbonatite metasomatism in the oceanic upper mantle. *Nature* **365**, 221–227.

Hawkesworth, C. J., Kempton, P. D., Rogers, N. W., Ellam, R. M. & van Calsteren, P. W. (1990). Continental mantle lithosphere and shallow mantle enrichment processes in the Earth's mantle. *Earth and Planetary Science Letters* **96**, 256–268.

Hoffman, P. F. (1990). Geological constraints on the origin of the mantle root beneath the Canadian Shield. *Philosophical Transactions of the Royal Society of London, Series A* **331**, 523–532.

Johnson, K. T. M., Dick, H. J. B. & Shimizu, N. (1990). Melting in the oceanic upper mantle: an ion microprobe study of diopsides in abyssal peridotites. *Journal of Geophysical Research* **95**, 2661–2678.

Jordan, T. H. (1988). Structure and formation of the continental tectosphere. *Journal of Petrology*, Special Lithosphere Issue, 11–37.

Kelemen, P. B., Hart, S. R. & Bernstein, S. (1998). Silica enrichment in the continental upper mantle via melt/rock reaction. *Earth and Planetary Science Letters* **164**, 387–406.

Kramers, J. D., Smith, C. B., Lock, N. P., Harmon, R. S. & Bory, F. R. (1981). Can kimberlites be generated from an ordinary mantle? *Nature* **291**, 53–56.

Kramers, J. D., Roddick, J. & Dawson, J. (1983). Trace element and isotope studies on veined, metasomatic and MARID xenoliths from Bultfontein, South Africa. *Earth and Planetary Science Letters* **65**, 90–106.

Lee, C.-T. & Rudnick, R. L. (2000). Compositionally stratified cratonic lithosphere: petrology and geochemistry of peridotite xenoliths from the Labait volcano, Tanzania. *Proceedings of the 7th International Kimberlite Conference* (in press).

Liu, D. Y., Nutman, A. P., Compston, W., Wu, J. S. & Shen, Q. H. (1992). Remnants of 3800 Ma crust in the Chinese part of the Sino-Korean craton. *Geology* **20**, 339–342.

Ma, X. Y. & Wu, D. (1981). Early tectonic evolution of China. *Precambrian Research* **14**, 185–202.

Maaloe, S. & Aoki, K. (1977). The major element composition of the upper mantle estimated from the composition of lherzolites. *Contributions to Mineralogy and Petrology* **63**, 161–173.

Mathias, M., Siebert, J. C. & Rickwood, P. C. (1970). Some aspects of the mineralogy and petrology of ultramafic xenoliths in kimberlite. *Contributions to Mineralogy and Petrology* **26**, 75–123.

McDonough, W. F. (1990). Constraints on the composition of the continental lithospheric mantle. *Earth and Planetary Science Letters* **101**, 1–18.

McDonough, W. F. & Frey, F. A. (1989). Rare earth elements in upper mantle rocks. In: Ribbe, P. H. (ed.) *Geochemistry and Mineralogy of Rare Earth Elements. Reviews in Mineralogy*, 99–145.

McDonough, W. F. & McCulloch, M. T. (1987). The southeast Australian lithospheric mantle: isotopic and geochemical constraints on its growth and evolution. *Earth and Planetary Science Letters* **86**, 327–340.

Menzies, M. A. (1991). Oceanic peridotites. In: Floyd, P. A. (ed.) *Oceanic Basalts*. Glasgow: Blackie, pp. 363–385.

Menzies, M. A. & Halliday, A. N. (1988). Lithospheric mantle domains beneath the Archaean and Proterozoic crust of Scotland. *Journal of Petrology* **29**, 275–302.

Menzies, M. A. & Murthy, V. R. (1980). Enriched mantle: Nd and Sr isotopes in diopsides from kimberlite nodules. *Nature* **283**, 634–636.

Menzies, M. A., Rogers, N., Tindle, A. & Hawkesworth, C. J. (1987). Metasomatic and enrichment processes in lithospheric peridotites, an effect of asthenosphere–lithosphere. In: Menzies, M. A. & Hawkesworth, C. J. (eds) *Mantle Metasomatism*. New York: Academic Press, pp. 312–364.

Menzies, M. A., Zhang, M. & Fan, W. (1993). Palaeozoic and Cenozoic lithoprobes and the loss of >120 km of Archaean Lithosphere Sino-Korean Craton China. In: Pritchard, H. M., Alabaster, T., Harris, N. B. W. & Neary, C. R. (eds) *Magmatic Processes and Plate Tectonics. Geological Society, London, Special Publication* **76**, 71–81.

Nelson, D. R., Chivas, A. R., Chappell, B. W. & McCulloch, M. T. (1988). Geochemical and isotopic systematics in carbonatites and

implications for the evolution of ocean-island sources. *Geochimica et Cosmochimica Acta* **52**, 1–17.

Pearson, D. G., Carlson, R. W., Shirey, S. B., Boyd, F. R. & Nixon, P. H. (1995*a*). Stabilisation of Archaean lithospheric mantle: a Re–Os isotope study of peridotite xenoliths from the Kaapvaal craton. *Earth and Planetary Science Letters* **134**, 341–357.

Pearson, D. G., Shirey, S. B., Carlson, R. W., Boyd, F. R., Pokhilenko, N. P. & Shimizu, N. (1995*b*). Re–Os, Sm–Nd and Rb–Sr isotope evidence for thick Archaean lithospheric mantle beneath the Siberian craton modified by multi-stage metasomatism. *Geochimica et Cosmochimica Acta* **59**, 959–977.

Peng, Z. C., Zartman, R. E., Futa, E. & Chen, D. G. (1986). Pb-, Sr- and Nd-isotopic systematics and chemical characteristics of Cenozoic basalts, eastern China. *Chemical Geology* **59**, 3–33.

Polet, J. & Anderson, D. A. (1995). Depth extent of cratons as inferred from tomographic studies. *Geology* **23**, 205–208.

Qi, Q., Taylor, L. A. & Zhou, X.-M. (1995). Petrology and geochemistry of mantle peridotite xenoliths from SE China. *Journal of Petrology* **36**, 55–79.

Richardson, S. H., Gurney, J. J., Erlank, A. J. & Harris, J. W. (1984). Origins of diamonds in old enriched mantle. *Nature* **310**, 198–202.

Richardson, S. H., Erlank, A. J. & Hart, S. R. (1985). Kimberlite-borne garnet peridotite xenoliths from old enriched subcontinental lithosphere. *Earth and Planetary Science Letters* **75**, 116–128.

Richardson, S. H., Harris, J. W. & Gurney, J. J. (1993). Three generations of diamonds from old continental mantle. *Nature* **366**, 256–258.

Rudnick, R., McDonough, W. F. & Orpin, A. (1994). Northern Tanzanian peridotite xenoliths: a comparison with Kaapvaal peridotites and inferences on metasomatic interactions. In: Meyer, H. O. A. & Leonardo, O. H. (eds) *Kimberlites, Related Rocks and Mantle Xenoliths. Proceedings of the 5th International Kimberlite Conference, 1*. Rio de Janeiro: Companhia de Pesquisa de Recursos Minerais, pp. 336–353.

Sen, G., Frey, F. A., Shimizu, N. & Leeman, W. P. (1993). Evolution of the lithosphere beneath Oahu, Hawaii: rare earth element abundances in mantle xenoliths. *Earth and Planetary Science Letters* **119**, 53–69.

Song, Y. & Frey, F. A. (1989). Geochemistry of peridotite xenoliths in basalt from Hannuoba, eastern China: implications for subcontinental mantle heterogeneity. *Geochimica et Cosmochimica Acta* **53**, 97–113.

Stosch, H. G. & Seck, H. A. (1980). Geochemistry and mineralogy of two spinel peridotite suites from Dreiser Weiher, West Germany. *Geochimica et Cosmochimica Acta* **44**, 457–470.

Tatsumoto, M., Basu, A. R., Huang, W. K., Wang, J. W. & Xie, G. H. (1992). Sr, Nd, and Pb isotopes of ultramafic xenoliths in volcanic rocks of Eastern China: enriched components EMI and EMII in subcontinental lithosphere. *Earth and Planetary Science Letters* **113**, 107–128.

Teng, J. W., Wang, Q. S., Liu, Y. C. & Wei, S. Y. (1983). Geophysical field characteristics, distribution and formation of hydrocarbon bearing basins of eastern China. *Journal of Geophysics* **26**(4), 319–330.

Van der Lee, S. & Nolet, G. (1997). Upper mantle S velocity structure of North America. *Journal of Geophysical Research* **102**, 22815–22838.

Walker, R. J., Carlson, R. W., Shirey, S. B. & Boyd, F. (1989). Os, Sr, Nd, and Pb isotope systematics of southern African peridotites xenoliths: implications for the chemical evolution of subcontinental mantle. *Geochimica et Cosmochimica Acta* **53**, 1583–1595.

Whitehouse, M. J., Windley, B. F. & Ba-B'ttat, M. A. (1994). Age and nature of continental crust in Yemen: new constraints on Pan-African crustal accretion rates. *US Geological Survey Circular* **1107**, 352 (abstract).

Xu, Y.-G., Menzies, M. A., Mattey, D. P., Lowry, D., Harte, B. & Hinton, R. W. (1996). The nature of the lithospheric mantle near the Tan-Lu fault, China: an integration of texture, chemistry and O-isotopes. *Chemical Geology* **134**, 67–81.

Xu, Y.-G., Menzies, M. A., Vroon, P., Mercier, J.-C. C. & Lin, C.-Y. (1998). Texture–temperature–geochemistry relationships in the upper mantle as revealed from spinel peridotite xenoliths from Wangqing, NE China. *Journal of Petrology* **39**, 469–493.

Xu, X., O'Reilly, S. Y., Griffin, W. L., Zhou, X. & Huang, X. (1998). The nature of the Cenozoic lithosphere of Nushan, eastern China. In: Flower, M. F. J., Chung, S.-L., Lo, C.-H. & Lee, T.-Y. (eds) *Mantle Dynamics and Plate Interactions in East Asia, Geophysical Monograph, American Geophysical Union Monograph*, **27**, 167–196.

Zhang, M., Menzies, M. A., Suddaby, P. & Thirlwall, M. F. (1991). EM1 signature from within post-Archaean subcontinental lithospheric mantle: isotopic evidence from the potassic volcanic rocks in NE China. *Geochemical Journal* **25**, 329–340.

Zhi, X., Song, Y., Frey, F. A., Feng, J. & Zhai, M. (1990). Geochemistry of Hannouba basalts, eastern China: constraints on the origin of continental alkalic and tholeiitic basalt. *Chemical Geology* **88**, 1–33.

Zhou, X. & Zhu, B. Q. (1992). Study on the isotopic system and mantle chemical zonation of Cenozoic basalt in eastern China. In: Liu, R. X. (ed.) *The Age and Geochemistry of Cenozoic Volcanic Rock in China*. Beijing: Seismologic Press, Beijing University, pp. 366–392.

Zhou, X. H. & Armstrong, R. L. (1982). Cenozoic volcanic rocks of eastern China—secular and geographic trends in chemistry and strontium isotopic composition. *Earth and Planetary Science Letters* **59**, 301–329.